Chemical Methodologies 3 (2019) 261-275

Chemical Methodologies

Journal homepage: http://chemmethod.com

Original Research article

Phthalimide Derivatives: New Promising Additives for Functional Electrolyte in Lithium-ion Batteries

Behrooz Mosallanejad

Department of chemistry, Amirkabir University of Technology, Tehran, Iran

ARTICLE INFORMATION

Received: 11 November 2018
Received in revised: 17 November 2018
Accepted: 25 November 2018
Available online: 26 November 2018

DOI: 10.22034/chemm.2018.155768.1109

KEYWORDS

Electrolyte additive
DFT computation
Solid electrolyte interface
Lithium-ion battery
Phthalimide derivatives

ABSTRACT

Vinylene carbonate (VC) is the most well-known additive for current lithium-ion batteries (LIBs). Low anodic stability or insufficient oxidation stability as a drawback of VC affected LIBs performance, especially in high voltage applications. As computational screening is faster and much less expensive than experimental trial and error testing, by using density functional theory (DFT) computations, phthalimide derivatives are screened as promising solid electrolyte interface (SEI) forming additives in LIBs. Our computational screening comprising frontier orbital energy, binding energy, and redox potentials shows that phthalimide derivatives are promising candidates as SEI-forming additives on graphite anode in ethylene carbonate (EC), and propylene carbonate (PC), based electrolytes. Additionally, four phthalimide derivatives including 3-nitrophthalimide, *N*-chlorophthalimide, 3,4,5,6-tetrachlorophthalimide, and phthalimide itself, due to their higher anodic stability and also reduction potential compared to VC, can be used as future alternatives of VC for LIBs.

*Corresponding author: E-mail: bmosallanejad@aut.ac.ir
Department of chemistry, Amirkabir University of Technology, Tehran, Iran, Tel: +98 910 646 5452

Graphical Abstract

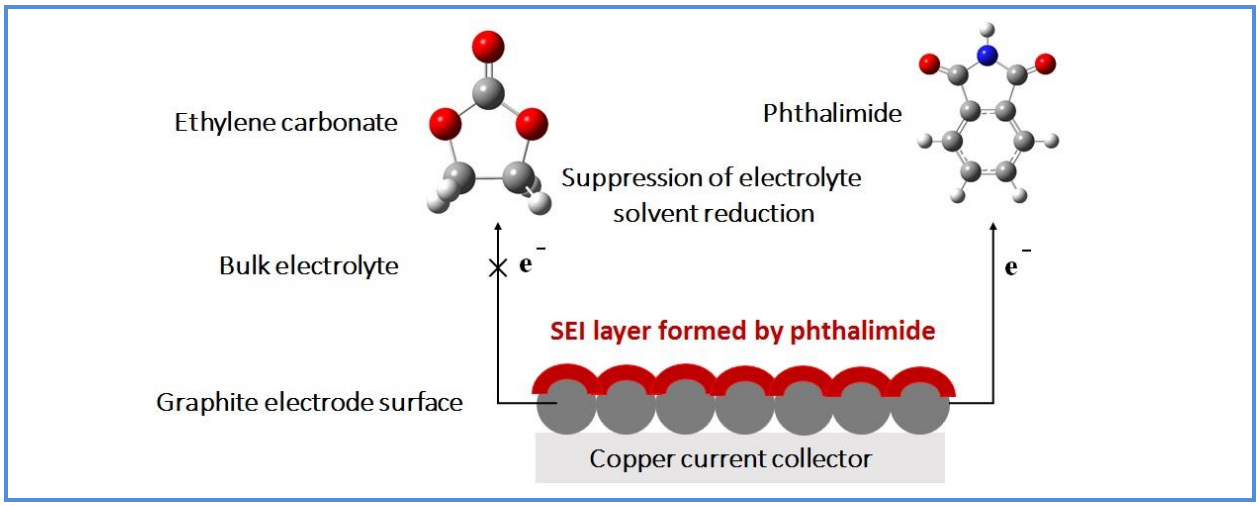

Introduction

Commercialization of lithium-ion batteries (LIBs) in 1991 by Sony corporation was the beginning of a wonderful development in electronic devices [1]. LIBs have extensively been used as power sources in portable electronic devices such as cell phones, laptop computers, and digital cameras due to their high energy density and high voltage; they also are promising energy sources for future transportation grid including electrical and hybrid electrical vehicles [2, 3]. The state of the art LIB consists of graphite anode, transition metal oxide cathode, electrolyte, separator, and current collectors (aluminium foil for cathode and copper foil for anode) [2]. Electrolyte as an essential element of LIBs includes a solvent or mixture of solvents as a medium for ionic conduction and a lithium salt as the solute for a source of lithium ion. Mixed solvent electrolyte comprises a cyclic alkyl carbonate like ethylene carbonate (EC) and propylene carbonate (PC) with high dielectric permittivity and linear alkyl carbonate such as dimethyl carbonate (DMC), diethyl carbonate (DEC), and ethyl methyl carbonate (EMC) with low viscosity which is essential for increasing the ionic conductivity of electrolyte [4, 5].

Solid electrolyte interface (SEI) is a passivation layer which is generally formed during the initial charging on the anode electrode of EC-based LIB due to the decomposition of electrolyte solvents and salt; because of exfoliation of graphite in PC-based electrolyte this issue is more significant [6, 7]. A conventional SEI consists of organic components like lithium salts of semi carbonates (also called alkyl carbonates) and some inorganic components such as Li_2CO_3, Li_2O, and LiF in $LiPF_6$-based electrolyte. Inorganic components act as insulators to both Li^+ ions and electrons [6-8]. There

are several ways not only to prevent SEI formation through consumption of solvent and salt in EC-based electrolyte but also inhibition of graphite anode's exfoliation through solvent co-intercalation in PC-based electrolyte. One of the most economic and effective methods is using the SEI-forming additives, also called "function-improving additives" [8]. Among these additives, vinylene carbonate (VC) is the most well-known additive used in LIBs was found in 1992 by Sanyo Electric Company. VC forms a stable SEI layer on the surface of anode to improve LIBs performance. Moreover, Ube Industries, Ltd. discovered that addition of small quantities of VC, can suppress PC decomposition at the graphite anode [9]. Low anodic stability or insufficient oxidation stability, is a drawback of VC, has recently been highlighted: during storage of LIBs in elevated temperature, the remaining VC in the electrolyte decomposes at the cathode and the adverse effects of VC maybe worsened in high voltage LIBs [10]. This has led to an extensive search for new additives which are superior to VC in anodic stability. Since computational screening is faster and much less expensive than experimental trial and error testing, so a screening approach *via* computational evaluation are used to identify new promising molecules as SEI additives [11, 12]. In this regard, Han and co-workers showed that fluoroethylene carbonate, trifluoromethyl propylene carbonate, methyl chloroformate, butane sultone, and chloroethylene carbonate are five promising SEI additives with high anodic stability comparable to fluoropropane sultone (FPS) [13]. According to the density functional theory (DFT)-based calculations of redox potentials and chemical reactivities with a hydrogen fluoride (HF) molecule of 35 phosphite derivatives, Han et al., proposed that trioleyl phosphite, tris(1-adamantyl) phosphite, distearyl pentaerythritol diphosphite, and tritertbutyl phosphite are promising candidates for successful cathode electrolyte interface (CEI)-forming electrolyte additives for use in high voltage LIBs [11]. Furthermore, Han et al., *via* screening of 32 lactam molecules as SEI additives for $LiCoO_2$/graphite cells found that *N*-acetyl caprolactam, *N*-acetyl *β*-propiolactam, *N*-acetyl glycine anhydride, and *N*-acetyl laurolactam have potential to use as SEI additives in LIB [12]. Some reports have experimentally confirmed the accuracy of prediction of DFT calculations. Jung et al., by using DFT calculations and electrochemical experiments reported that FPS outperforms VC and 1,3-propane sultone (PS) because of its higher anodic stability and excellent SEI-forming ability [10]. The theoretical and experimental results obtained from Han's et al., work showed that tris(trimethylsilyl) phosphite (TMSP) is oxidized more readily and is reduced more difficultly than an electrolyte solvent and also exhibits high reactivity with HF [14].

Phthalimide is an organic compound with the formula $C_6H_4(CO)_2NH$ that is a derivative of phthalic anhydride [15–17]. In this work, for the first time, we intended to investigate 22 phthalimide derivatives as SEI additives in LIBs. phthalimide derivatives can be divided into two groups

according to the substituent position; in the first group, the hydrogen bonded to the nitrogen is exchanged with different functional groups, called "imide position" and in another one, the positions which hydrogens bonded to the benzene ring called "phenyl position" (Figure 1).

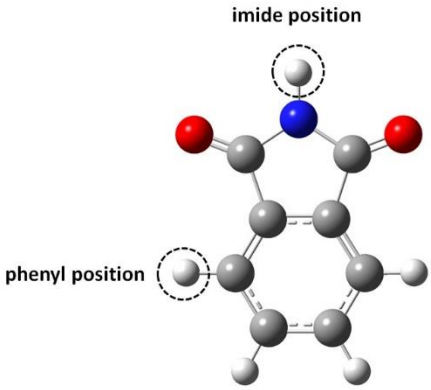

Figure 1. Imide and phenyl positions in the phthalimide molecule

The molecular structures of phthalimide derivatives attended in this work are shown in Figure 2.

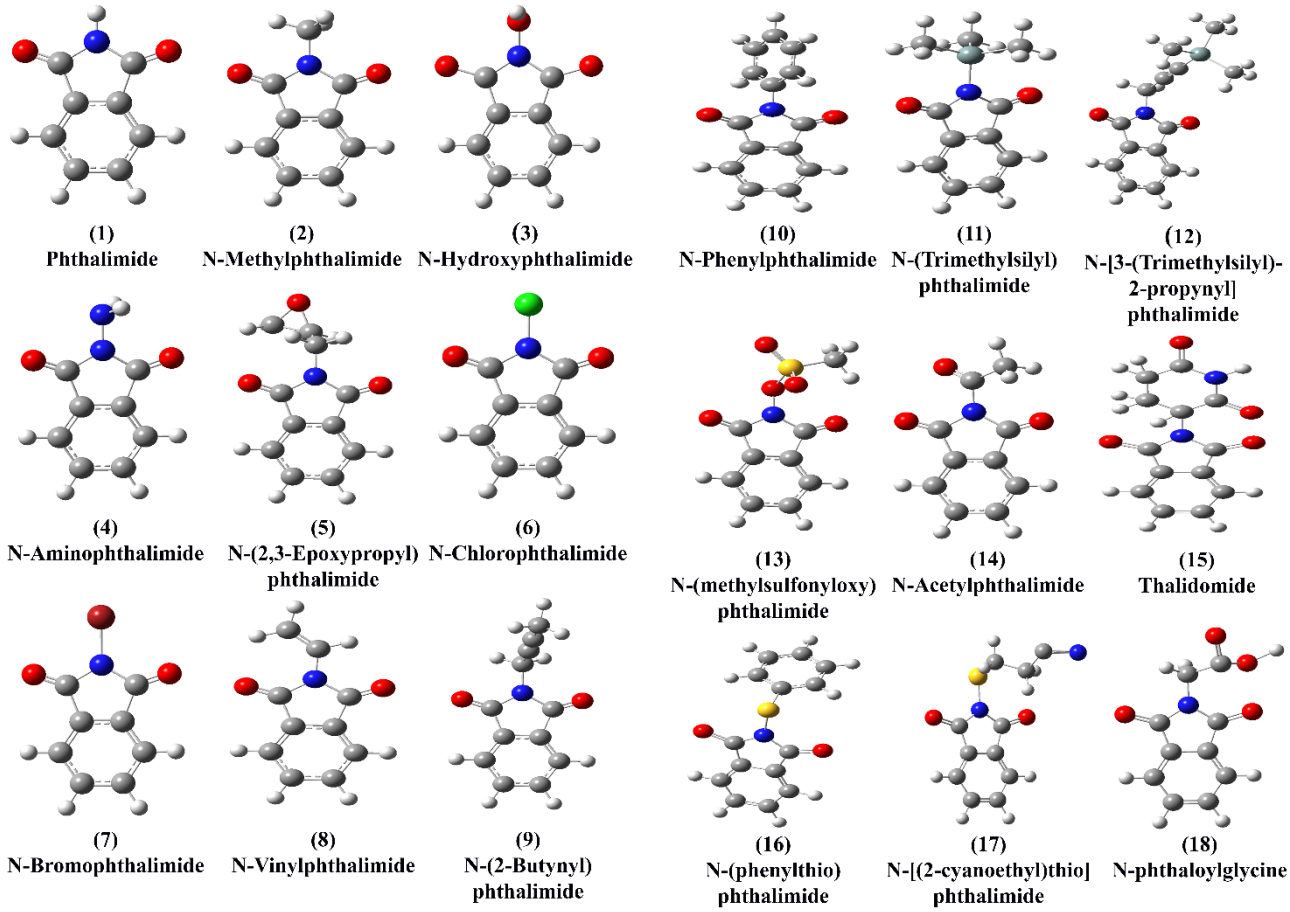

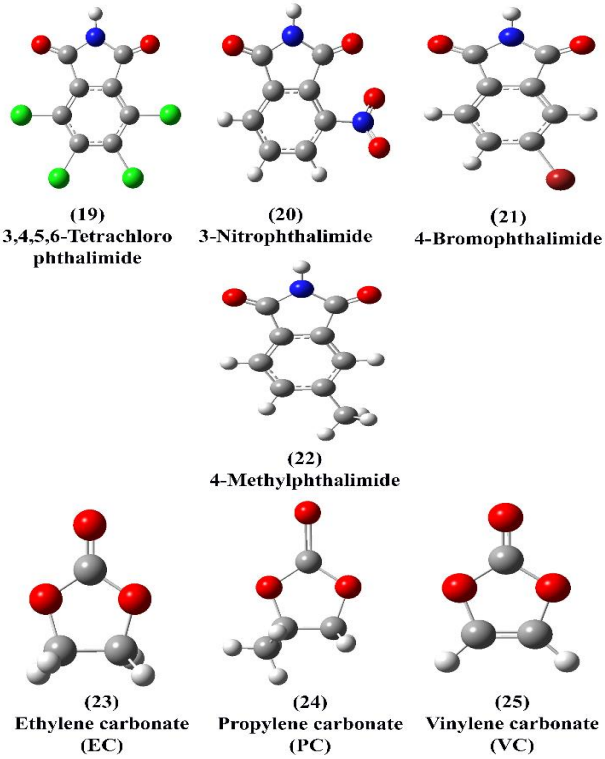

Figure 2. The chemical structures of EC, PC, VC, and phthalimide derivatives

In this study, it is considered that each of the phthalimide derivatives are available from Sigma-Aldrich. In this regard, for computational screening of phthalimide derivatives, three parameters are considered: (1) frontier orbital energy, (2) binding energy, and (3) redox potentials (Figure 3).

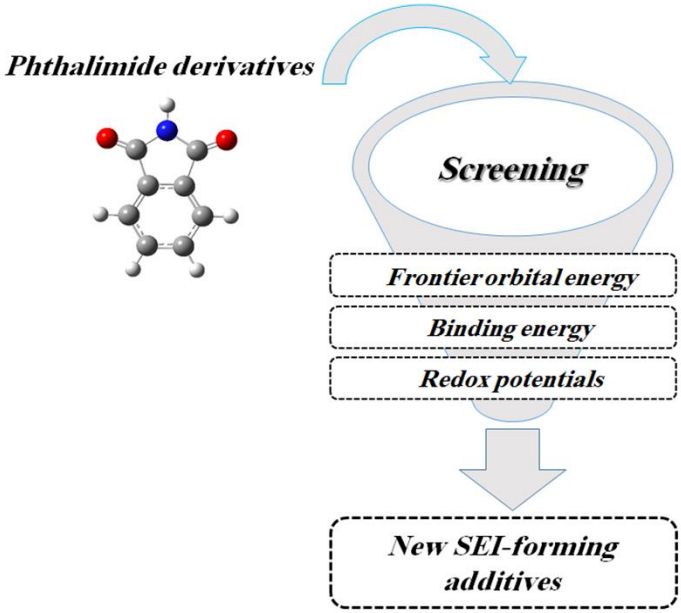

Figure 3. The parameters used for screening of phthalimide derivatives

Experimental

Computational Methods

Calculation of molecular properties of a vast array of organic molecules that are used in LIBs is done by Kohn-Sham DFT method [18]. The optimized structures of the molecules which are shown in Figure 2. were obtained with C1 symmetry, B3PW91 functional and 6-311G(d,p) basis sets of triple-ζ quality as implemented in program package Gaussian 09 [19]. The B3PW91 functional consists of a linear combination of the exact Hartree-Fock exchange, Slater exchange [20], and B88 gradient-corrected exchange [21] that are a three-parameter adiabatic connection exchange term [22]. A conductor-variant polarized continuum model (CPCM) [23], was adopted to place the solute in a molecular-shaped cavity embedded in a continuum dielectric medium. As EC: EMC= 1:2 electrolyte solution is widely used in LIBs, so a dielectric constant of 31.9 was employed as a weighted average value between the dielectric constant of EC (ε=89.2) and EMC (ε=2.9) [5-24].

Results and Discussion

Frontier orbital energy

Highest occupied molecular orbital energy (E_{HOMO}) and lowest unoccupied molecular orbital energy (E_{LUMO}) represent the ability of a molecule to undergo oxidation and reduction reaction, respectively [14-25]. The energy difference between HOMO and LUMO levels, termed HOMO-LUMO gap, is a parameter for measuring the reactivity of a molecule, defined by following equation:

$$\Delta E_g^a = E_{LUMO} - E_{HOMO} \quad (1)$$

A large HOMO-LUMO gap corresponds to high stability of a molecule and low reactivity toward chemical reaction [26]. A SEI additive is suggested to have lower E_{LUMO} and E_{HOMO} than that of the electrolyte solvent (Figure 4a). These two parameters enable the additive to form an effective SEI layer on the surface of negative electrode prior to the solvent reduction without any adverse reaction on cathode [25-27].

The E_{HOMO}, E_{LUMO}, and ΔE_g^a of EC, PC, VC, and phthalimide derivatives are presented in Table 1.

Table 1. The E_{HOMO}, E_{LUMO} and ΔE_g^a of EC, PC, VC, and phthalimide derivatives

No.	Material	HOMO (eV)	LUMO (eV)	ΔE_g^a(eV)
1	Phthalimide	-7.73	-2.55	5.18
2	*N*-Methylphthalimide	-7.50	-2.52	4.98
3	*N*-Hydroxyphthalimide	-7.62	-2.67	4.95
4	*N*-Aminophthalimide	-7.57	-2.56	5.01
5	*N*-(2,3-Epoxypropyl)phthalimide	-7.48	-2.59	4.89
6	*N*-Chlorophthalimide	-7.61	-2.81	4.8
7	*N*-Bromophthalimide	-7.49	-2.76	4.73
8	*N*-Vinylphthalimide	-6.90	-2.67	4.23
9	*N*-(2-Butynyl)phthalimide	-7.41	-2.59	4.82
10	*N*-Phenylphthalimide	-7.44	-2.57	4.87
11	*N*-(Trimethylsilyl)phthalimide	-7.53	-2.44	5.09
12	*N*-[(3-(Trimethylsilyl)-2-propynyl]phthalimide	-7.55	-2.61	4.94
13	*N*-(Methylsulfonyloxy)phthalimide	-7.77	-2.87	4.9
14	*N*-Acetylphthalimide	-7.56	-2.73	4.83
15	Thalidomide	-7.53	-2.70	4.83
16	*N*-(Phenylthio)phthalimide	-7.29	-2.65	4.64
17	*N*-[(2-Cyanoethyl)thio]phthalimide	-7.31	-2.71	4.59
18	*N*-Phthaloylglycine	-7.64	-2.61	5.03
19	3,4,5,6-Tetrachlorophthalimide	-7.63	-3.10	4.53
20	3-Nitrophthalimide	-7.91	-3.10	4.81
21	4-Bromophthalimide	-7.41	-2.71	4.7
22	4-Methylphthalimide	-7.40	-2.47	4.93
23	Ethylene carbonate (EC)	-8.49	0.71	9.2
24	Propylene carbonate (PC)	-8.46	0.75	9.21
25	Vinylene carbonate (VC)	-7.13	-0.01	7.12

All of the phthalimide derivatives have lower E_{LUMO} than that of EC (or PC), which means that these molecules are expected to reduce prior to the reduction of solvent and form SEI layer, but, these molecules have higher E_{HOMO} than that of EC (or PC), reflecting phthalimide derivatives have lower anodic stability and they are oxidized before solvent on cathode. It is worth to note that all of molecules have lower E_{LUMO} than that of VC, therefore, they show better SEI layer forming ability

compared with VC. Also, these molecules except *N*-vinylphthalimide (additive 8) have lower E_{HOMO} which exhibit higher anodic stability than that of VC.

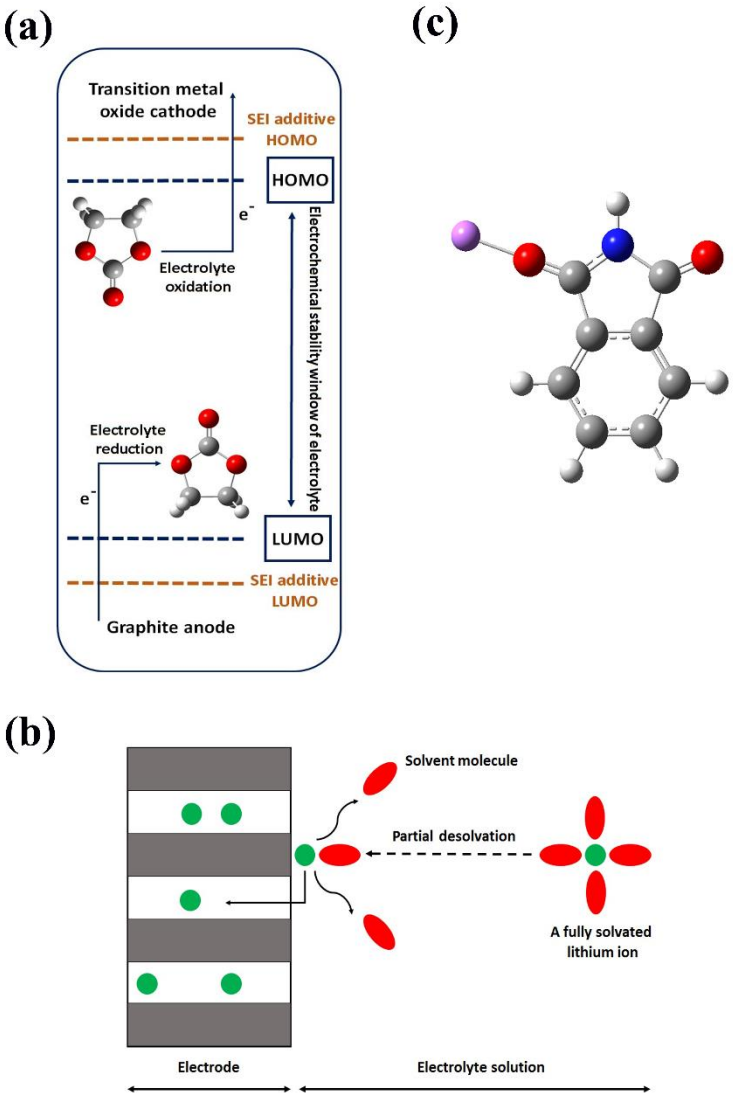

Figure 4. (a) The SEI and CEI formation processes on the anode and cathode surfaces respectively, (b) schematic representation of mechanism of Li^+ ion intercalation into the electrode, (c) the optimized structure of the phthalimide bonded to a Li^+ ion

Binding energy

Low Li^+ binding energy is another important parameter in screening of SEI additives. The reason of low binding energy is that the desolvation process or stripping of solvation sheath of Li^+ ion in the intercalation process of Li^+ ion into the electrode is a major energy-consuming step in LIBs, so, the weak binding of the molecule with Li^+ ion facilitates the desolvation reaction (Figure 4b) [28].

The molecules 3, 4, 6, and 13 from imide position with the lowest E_{HOMO} among the molecules, phthalimide as the base molecule and phenyl position molecules (molecules 19, 20, 21, and 22) are nine molecules selected for binding energy and redox potentials investigations. Table 2 shows the binding energies of molecules in gas and solution phases.

Table 2. Binding energies of molecules in gas and solution phases

Material	Binding energy BE(Li^+) (eV)	
	Gas	Solvent
(1) Phthalimide	2.05	0.19
(3) *N*-Hydroxyphthalimide	2.38	0.21
(4) *N*-Aminophthalimide	2.00	0.18
(6) *N*-Chlorophthalimide	2.01	0.16
(13) *N*-(Methylsulfonyloxy)phthalimide	2.86	0.14
(19) 3,4,5,6-Tetrachlorophthalimide	2.1	0.15
(20) 3-Nitrophthalimide	1.79	0.15
(21) 4-Bromophthalimide	1.96	0.17
(22) 4-Methylphthalimide	2.29	0.19
(23) Ethylene carbonate (EC)	2.24	0.24
(24) Propylene carbonate (PC)	2.32	0.26
(25) Vinylene carbonate (VC)	2.06	0.20

Binding energy is calculated by subtracting the ground-state energies of target molecule and Li^+ ion from the singly coordinated Li^+-molecule which the Li^+ ion is located in a 180° position with respect to the carbonyl group of each target molecule (Figure 4c) [29]. Except for binding energies of molecules 3, 13, and 22 in the gas phase which are higher than that of EC (and molecules 3 and 13 with respect to PC), others have lower binding energies in both of gas and solution phases compared with EC (or PC). That is, the connection of Li^+ ion with these molecules is weaker than that of electrolyte solvent and the desolvation needs lower energy to occur in the intercalation process.

Redox potentials

Oxidation Gibbs free energy (ΔG_{ox}) and reduction Gibbs free energy (ΔG_{red}) represent anodic and cathodic stability of a molecule, respectively. The first requirement for the SEI additive is to have lower ΔG_{red} or higher reduction potential (RP) than that of the electrolyte solvent. That is, the additive is easily reduced prior to the reduction of solvent and formed SEI film on the negative

electrode surface. Furthermore, the additive is suggested to have higher anodic stability than that of the solvent, which requires to have the higher ΔG_{ox} or higher oxidation potential (OP) [10]. The Born-Haber cycle given in scheme 1. is used to calculate the Gibbs free energy of redox half reaction $\Delta G^{\circ,redox}_{solv}$ and OP of a reductant (Red) relative to an electron at rest in vacuum $E^{\circ}_{abs}(Red)$, which are expressed by equations 2 and 3, respectively:

$$\Delta G^{\circ,redox}_{solv} = \Delta G^{\circ,redox}_{gas} + \Delta G^{\circ}_{s}(Ox) - \Delta G^{\circ}_{s}(Red) \quad (2)$$

$$E^{\circ}_{abs}(Red) = \Delta G^{\circ,redox}_{solv}/F \quad (3)$$

$$E^{\circ}\left(vs\ \frac{L^{+}}{Li}\right) = E^{\circ}_{abs} - 1.37\ V \quad (4)$$

$\Delta G^{\circ,redox}_{gas}$ is the ionization free energy in the gas phase at 298.15 K, $\Delta G^{\circ}_{s}(Ox)$ and $\Delta G^{\circ}_{s}(Red)$ are the free energies of the oxidant (Ox) and Red molecules respectively, and F is the Faraday constant. Equation 4 is used to convert the absolute oxidation potential to the Li^{+}/Li scale [30, 31].

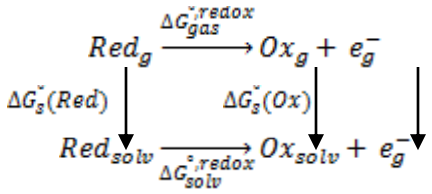

Scheme 1. The Born-Haber cycle for calculation of oxidation potential

Like calculation of OP, the Born-Haber cycle shown in scheme 2. is used to calculate the RP [32].

$$\Delta G^{\circ,redox}_{solv} = \Delta G^{\circ,redox}_{gas} + \Delta G^{\circ}_{s}(Red) - \Delta G^{\circ}_{s}(Ox) \quad (5)$$

$$E^{\circ}_{abs}(Ox) = -\Delta G^{\circ,redox}_{solv}/F \quad (6)$$

Equations 5 and 6 are used to calculate Gibbs free energy of redox half reaction $\Delta G^{\circ,redox}_{solv}$ and RP of an Ox relative to an electron at rest in vacuum $E^{\circ}_{abs}(Ox)$, respectively. equation 4 is also used to convert the absolute RP to the Li^{+}/Li scale.

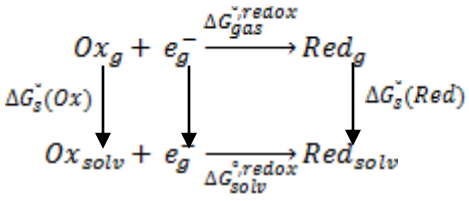

Scheme 2. The Born-Haber cycle for calculation of reduction potential

Gibbs free energies and redox potentials of chosen phthalimide derivatives are shown in Table 3.

Table 3. The Gibbs free energies and redox potentials of molecules

Material	Gibbs free energy (kJ/mol)		Redox potential (eV)	
	ΔG_{red}	ΔG_{ox}	RP	OP
(1) Phthalimide	-279.94	716.51	1.53	6.05
(3) *N*-Hydroxyphthalimide	-291.47	661.92	1.65	5.49
(4) *N*-Aminophthalimide	-280.76	586.2	1.54	4.70
(6) *N*-Chlorophthalimide	-305.06	709.57	1.79	5.98
(13) *N*-(Methylsulfonyloxy) phthalimide	-309.34	692.83	1.83	5.81
(19) 3,4,5,6-Tetrachlorophthalimide	-333.32	707.49	2.08	5.96
(20) 3-Nitrophthalimide	-286.28	724.09	1.59	6.13
(21) 4-Bromophthalimide	-296.11	696.13	1.69	5.84
(22) 4-Methylphthalimide	-277.03	684.09	1.50	5.72
(23) Ethylene carbonate (EC)	-98.05	803.87	-0.35	6.96
(24) Propylene carbonate (PC)	-96.14	795.21	-0.37	6.87
(25) Vinylene carbonate (VC)	-129.74	674.17	-0.02	5.62

Results show that all of the molecules have higher RP than that of EC (or PC), so, these molecules have the potential to be employed as SEI additives for graphite anode in EC and also PC-based electrolytes.

Interestingly, these molecules have lower cathodic stability compared to VC, that is, they show better performance in SEI formation on the anode surface. In addition to the higher RP, the chosen phthalimide derivatives have lower OP with respect to EC (or PC). It clearly reflects that these materials have lower anodic stability than that of solvent and oxidized before that. The remarkable thing is that these molecules except 3 and 4 have more anodic stability than that of VC. As a summing up, a suitable SEI additive is suggested to have the parameters are shown in Figure 5. respect to electrolyte solvent.

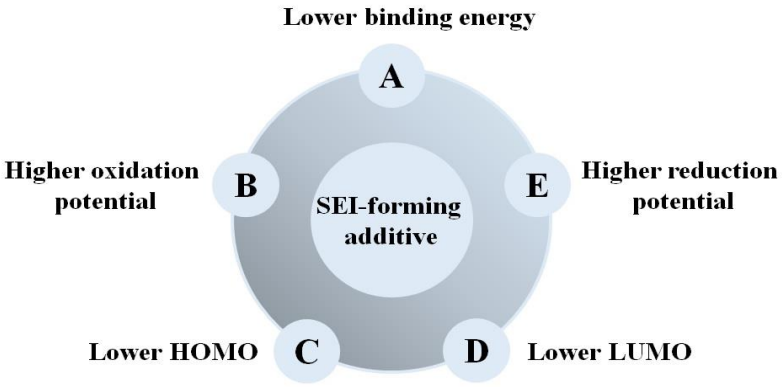

Figure 5. The parameters that a SEI additive is suggested to have respect to electrolyte solvent

Correlation between frontier orbital energy and redox potentials

Figure 6. displays correlations between E_{HOMO} and OP as well as E_{LUMO} and RP values. The correlation coefficient between E_{HOMO} and OP is 0.5931 while between E_{LUMO} and RP is 0.9803, meaning that correlation between E_{HOMO} and OP is very weak. As a result, for an accurate determination of oxidation and reduction abilities of additives, measuring redox potentials is more preferred instead of frontier orbital energy [12-14].

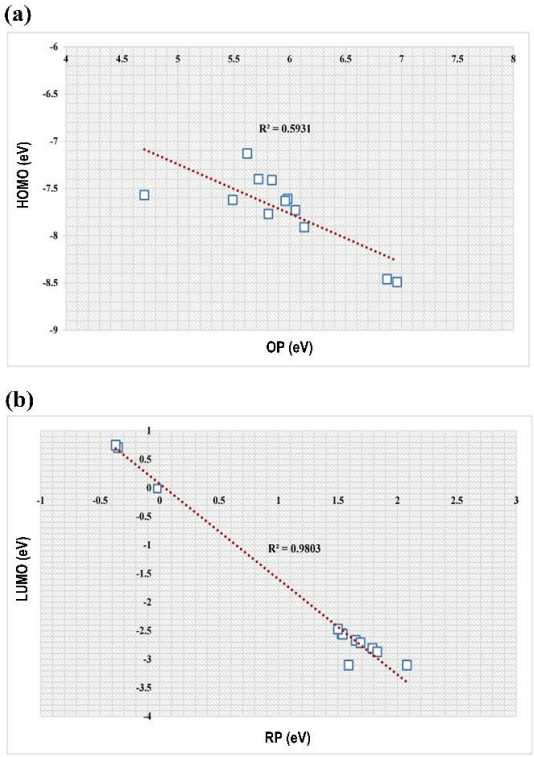

Figure 6. Correlation between (a) E_{HOMO} and oxidation potential (OP) and (b) E_{LUMO} and reduction potential (RP) (The R^2 values are correlation coefficients)

Conclusion

In this work, the SEI formation ability of phthalimide derivatives was investigated. Highlights of this work are:

1. Because of the frontier orbital energy, binding energy, and redox potentials of phthalimide derivatives showed good results, these materials can be candidate as promising SEI-forming additives on graphite anode and also can be used in PC-based electrolyte to suppress exfoliation of graphite.

2. Since some of phthalimide derivatives like 3-nitrophthalimide, *N*-chlorophthalimide, 3,4,5,6-tetrachlorophthalimide, and phthalimide itself significantly showed higher anodic stability compared to the VC, therefore, the drawback of VC due to its insufficient oxidation stability can be solved by using of these additives.

3. Correlation results showed that redox potentials in comparison to frontier orbital energy are more preferred parameters for determining new SEI additives.

Acknowledgements

The financial support of this work by Research Office of Amirkabir University of Technology (Tehran Polytechnic) is gratefully acknowledged.

References

[1] Nishi Y. *J. Power Sources,* 2001, **100**:101

[2] Haregewoin A.M., Wotango A.S., Hwang B.J. *Energy Environ. Sci.,* 2016, **9**:1955

[3] Korepp C., Kern W., Lanzer E.A., Raimann P.R., Besenhard J.O., Yang M., Möller K.C., Shieh D.T., Winter M. *J. Power Sources,* 2007, **174**:637

[4] Zhang Z., Zhang S.S. *Rechargeable Batteries*; Springer: Switzerland, 2015; p 263

[5] Xu K. *Chem. Rev.,* 2004, **104**:4303

[6] Choi N., Chen Z., Freunberger S.A., Ji X., Sun Y.K., Amine K., Yushin G., Nazar L.F., Cho J., Bruce P.G. *Angew. Chem. Int. Ed.,* 2012, **51**:9994

[7] Yao W., Zhang Z., Gao J., Li J., Xu J., Wang Z., Yang Y. *Energy Environ. Sci.,* 2009, **2**:1102

[8] Zhang S.S. *J. Power Sources,* 2006, **162**:1379

[9] Jow T.R., Xu K., Borodin O., Makoto U. *Electrolytes for lithium and lithium-ion batteries*; Springer: New York, 2014; p 167

[10] Jung H.M., Park S.-H., Jeon J., Choi Y., Yoon S., Cho J.J., Oh S., Kang S., Han Y.K., Lee H. *J. Mater. Chem. A,* 2013, **38**:11975

[11] Han Y.K., Yoo J., Yim T. *RSC Adv.,* 2017, **7**:20049

[12] Han Y.K., Moon Y., Lee K., Huh Y.S. *Curr. Appl. Phys.,* 2014, **14**:897

[13] Han Y.K., Lee K., Jung S.C., Huh Y.S. *Comput. Theor. Chem.,* 2014, **1031**:64

[14] Han Y.K., Yoo J., Yim T. *J. Mater. Chem. A,* 2015, **3**:10900

[15] Sabastiyan A., Suvaikin M.Y. *Adv. Appl. Sci. Res.,* 2012, **3**:45

[16] Kushwaha N., Kaushik D. *J. Appl. Pharm. Sci.,* 2016, **6**:159

[17] Kushwaha N., Tripathi A., Kushwaha S.K.S. *Der Pharm. Chem.,* 2014, **6**:188

[18] Kümmel S., Kronik L. *Rev. Mod. Phys.,* 2008, **80**:3

[19] Frisch M.J., Trucks G.W., Schlegel H.B., Scuseria G.E., Robb M.A., Cheeseman J.R., Scalmani G., Barone V., Mennucci B., Petersson G.A., Nakatsuji H., Caricato M., Li X., Hratchian H.P., Izmaylov A.F., Bloino J., Zheng G., Sonnenberg J.L., Hada M., Ehara M., Toyota K., Fukuda R., Hasegawa J., Ishida M., Nakajima T., Honda Y., Kitao O., Nakai H., Vreven T., Montgomery Jr.J.A., Peralta J.E., Ogliaro F., Bearpark M., Heyd J.J., Brothers E., Kudin K.N., Staroverov V.N., Kobayashi R., Normand J., Raghavachari K., Rendell A., Burant J.C., Iyengar S.S., Tomasi J., Cossi M., Rega N., Millam J. M., Klene M., Knox J.E., Cross J.B., Bakken V., Adamo C., Jaramillo J., Gomperts R., Stratmann R.E., Yazyev O., Austin A.J., Cammi R., Pomelli C., Ochterski J.W., Martin R.L., Morokuma K., Zakrzewski V.G., Voth G.A., Salvador P., Dannenberg J.J., Dapprich S., Daniels A.D., Farkas O., Foresman J.B., Ortiz J.V., Cioslowski J., Fox D.J. Gaussian 09, Revision A.02, Gaussian, Inc., Wallingford CT, 2009.

[20] Vosko S. H., Wilk L., Nusair M. *Can. J. Phys.*, 1980, **58**:1200

[21] Becke A.D. *Phys. Rev. A*, 1988, **38**:3098

[22] Becke A.D. *J. Chem. Phys.,* 1993, **98**:5648

[23] Barone V., Cossi M., Tomasi J. *J. Comput. Chem.,* 1998, **19**:404

[24] Zhang S.S., Jow T.R., Amine K., Henriksen G.L. *J. Power Sources,* 2002, **107**:18

[25] Halls M.D., Tasaki K. *J. Power Sources,* 2010, **195**:1472

[26] Chen R., Wu F., Li L., Guan Y., Qiu X., Chen S., Li Y., Wu S. *J. Power Sources,* 2007, **172**:395

[27] Abe K., Miyoshi K., Hattori T., Ushigoe Y., Yoshitake H. *J. Power Sources,* 2008, **184**:449

[28] Park M.H., Lee Y.S., Lee H., Han Y.-K. *J. Power Sources*, 2011, **196**:5109

[29] Klassen B., Aroca R., Nazri M., Nazri G.A. *J. Phys. Chem. B*, 1998, **102**:4795

[30] Borodin O., Behl W., Jow T.R. *J. Phys. Chem. C*, 2013, **117**:8661

[31] Trasatti S. *Pure Appl. Chem.,* 1986, **58**:955

[32] Leggesse E.G., Jiang J.C. *J. Phys. Chem. A,* 2012, **116**:11025

How to cite this manuscript: Behrooz Mosallanejad. Phthalimide Derivatives: New Promising Additives for Functional Electrolyte in Lithium-ion Batteries. Chemical Methodologies 3(2), 2019, 261-275. DOI:**10.22034/chemm.2018.155768.1109.**